



13 **Abstract**

14 By considering the moisture transport for precipitation (MTP) for a target region to be the moisture that arrives
15 in this region from its major moisture sources and which then results in precipitation in that region, we explore
16 i) whether the MTP from the main moisture sources for the Arctic region is linked with interannual fluctuations
17 in the extent of Arctic Sea ice superimposed on its decline and ii) the role of extreme MTP events in the inter-
18 daily change of the Arctic Sea Ice Extent (SIE) when extreme MTP simultaneously arrives from the four main
19 moisture regions that supply it. The results suggest 1) that ice-melting at the scale of interannual fluctuations
20 against the trend is favoured by an increase in moisture transport in summer, autumn, and winter, and a
21 decrease in spring and, 2) on a daily basis, extreme humidity transport increases the formation of ice in winter
22 and decreases it in spring, summer and autumn; in these 3 seasons it therefore contributes to Arctic Sea Ice
23 Melting. These patterns differ sharply from that linked to the decline, especially in summer when the opposite
24 trend applies.

25

26 **Keywords:** *Arctic Sea Ice, Atmospheric moisture transport, precipitation, interannual fluctuations, interdaily*
27 *fluctuations, Lagrangian approach*

28

29 **1 Introduction**

30 If the scientific community were collectively to select an unambiguous indicator of climate change, the long-
31 term decline in the average annual extent of Arctic sea ice (SIE) would undoubtedly be among the most widely
32 proposed. This is not just because of the extreme levels of social concern that this topic generates (IPCC,
33 2013) in view of all the considerable environmental implications, but also because the scientific complexity
34 of this field of study covers a very broad spectrum of disciplines. These range from atmospheric and oceanic
35 sciences related to the origins and processes of the sea ice, to marine biology and even economics and energy
36 resources (IPCC, 2013), all related to the study of the consequences of any change.

37

38 One of the most influential atmospheric mechanisms affecting the Arctic SIE, and one which has received the
39 most attention, is the transport of moisture from mid-latitudes. A number of authors (e.g., Dufour et al, 2016;
40 Oshima and Yamazaki, 2017) have found no significant long-term changes in the poleward moisture transport
41 towards the Arctic, while others (e.g., Zhang et al, 2012) noted an intensification of this transport over the last
42 few decades. A change in moisture transport towards the Arctic is relevant in two senses, in that it provides
43 more humidity into the Arctic with a consequent increase in the radiative forcing of water vapour, which in



44 turn contributes to increased melting of the ice, but also in that it can contribute to a change in the patterns of
45 rainfall over the Arctic.

46

47 The first of these two effects has undoubtedly attracted more attention of late. More moisture transport into
48 the Arctic may induce anomalous long-wave downward radiation at the surface, warming of the atmospheric
49 column, and a decrease in Arctic ice (e.g., Woods and Caballero, 2016). At a seasonal scale, Kapsch et al.
50 (2013) showed a greater transport of humidity towards the Arctic in the winter and the preceding spring (in
51 those years when there is a low concentration of sea ice in the Arctic in summer). Much attention has also
52 been focused on the role of extreme moisture transport events, both in winter (e.g., Woods et al, 2013; Park et
53 al., 2015) and spring (e.g., Yang and Magnusdottir, 2017), with similar conclusions in both cases that extreme
54 events are accompanied by a reduction in the concentration of sea ice.

55

56 The second effect occurs via the impact of changes in moisture transport in Arctic precipitation and is more
57 complex because changes in precipitation can cause different changes in ice cover associated with different
58 fusion mechanisms depending on the form of precipitation (rain or snow), as well as its intensity and
59 seasonality (Vihma, 2016).

60

61 In our previous work (Gimeno-Sotelo et al, 2018) we addressed the changes in patterns of MTP linked to the
62 annual mean decline by comparing two periods (before vs. after the major change point in 2003). However,
63 some substantial high-frequency interannual fluctuations are also superimposed on this negative trend, and
64 these modulate the annual observations of SIE, but have attracted less attention. Additionally, to our knowledge
65 the role of extreme MTP events on the daily march of SIE has never been analysed.

66

67 In this article we complement our previous study by i) focusing on the pattern of MTP linked to high-frequency
68 interannual variability as characterized by years with low / high SIE set against its long-term decline and ii)
69 analysing the role of extreme MTP events in the Arctic SIE by investigating what happens to the daily march
70 of the Arctic Sea ice extent when extreme MTP transport periods from the four main sources of humidity for
71 the Arctic coincide.

72

73



74 **2 Data and Methods**

75 The Arctic region (AR) and its four main sources of moisture (Figure 1a), and the Arctic Ocean (AO) and its
76 sub-regions (Figure 1b), are the same as used in our previous study (Gimeno-Sotelo 2018). The boundary of
77 the AR was defined by Roberts et al. (2010), and the moisture sources were defined by Vazquez et al (2016).
78 The study covers the period from January 1, 1980 to December 31, 2016, and the daily data on the Arctic SIE
79 were obtained from the USA National Snow and Ice Data Center (Fetterer, 2016). Data from the European
80 Centre for Medium-Range Weather Forecasts (ECMWF) reanalysis (ERA-Interim) (Dee et al., 2011) were
81 used to drive the Lagrangian moisture transport model and to calculate the vertical integrated moisture flux.
82 This reanalysis contains data since 1979 at six-hour intervals with a spatial resolution of $1^\circ \times 1^\circ$ in latitude
83 and longitude with 61 vertical levels (1000 to 0.1 hPa). It is considered to be the reanalysis that best represents
84 the hydrological cycle (Lorenz and Kunstmann, 2012), being particularly useful for studies of the Arctic region
85 (Jakobson et al., 2012; Graversen et al., 2011).

86

87 The Lagrangian approach used to calculate the MTP is that used by Stohl and James 2004; 2005, based on the
88 FLEXPART particle dispersion model in which the atmosphere is divided in finite elements of volume of
89 equal mass, which we call particles, and their trajectory is traced for a period of ten days, normally used as
90 the average time that water vapour resides in the troposphere (Numaguti, 1999). The specific moisture
91 changes of the particles are used to estimate the total budget of atmospheric humidity, or Evaporation minus
92 Precipitation (E-P), by adding up all these changes in specific humidity for all the particles in a given area.
93 By choosing all the particles that a) leave a given source region, b) reach the AR, and c) lose humidity in the
94 AR, we can calculate the MTP from the source region to the AR for a given daily, monthly, or yearly time
95 scale by adding these losses of specific humidity for all these particles. This Lagrangian method has been used
96 extensively and successfully in the analysis of moisture sources and sinks (e.g., Gimeno et al., 2010; 2013)
97 and is considered state-of-the-art compared with other methods of tracing water vapour (Gimeno et al., 2012;
98 2016).

99

100 **3. Overview of moisture transport to the Arctic**

101 A general scheme of the moisture transport to the Arctic can be extracted from the climatological values of
102 vertical integrated moisture flux (VIMF) throughout the year. Figure 2 illustrates these values for the first
103 month of each season together with the main Arctic sources identified by Vázquez et al (2016), the AR and
104 the main sub-regions of the AO in terms of moisture received from the source regions (Figure S1 in the



105 supplementary material shows the 12 months). These figures are useful for visualizing some of the most
106 pertinent results from our previous studies, namely:

107 i) The Pacific, North America, Siberia, and the Atlantic sources contribute to the moisture received in the AR
108 in about 35, 30, 20, and 15 %, respectively, being the relative importance of the four moisture sources
109 relatively constant throughout the year, with the Pacific, North America, Siberia, and the Atlantic contributing
110 about 35, 30, 20, and 15 %, respectively (Gimeno-Sotelo et al., 2018).

111 ii) there are four sub-regions of the AO (Baffin Bay, the Bering Sea, Greenland, and the central Arctic, shown
112 in the Figure 2), which receive most of the moisture reaching the AO from the four main sources, with small
113 variations throughout the year for Baffin Bay, the Bering Sea, and the central Arctic, but with a marked
114 seasonal cycle for Greenland (Gimeno-Sotelo et al, 2018).

115 iii) the Atlantic source is dominant in the Bering and Greenland subregions, the Pacific source dominates in
116 the Barents, and all four sources contribute to the central Arctic (Vázquez et al., 2016).

117

118 **4 Results**

119 ***4.1 Patterns of moisture transport for precipitation linked to high-frequency interannual fluctuations of*** 120 ***the Arctic sea ice extent***

121 To separate the superimposed high-frequency interannual fluctuations from the long-term decline in the Arctic
122 SIE, we divided the annual mean time series for each month into low- and high-frequency components as per
123 *Yang and Magnusdottir (2017)*. Figure 3 illustrates this approach by showing the monthly May Arctic ice
124 extent series for the AR from 1980 to 2016 (black line), together with a filtered series using a 10-year moving
125 mean (obtained by substituting each value with the mean of the five previous, the five subsequent values, and
126 the value itself, shown by the green line). Two blue lines are also plotted: a solid one obtained by adding the
127 standard deviations of the non-filtered series to each of the values of the filtered series, and a dotted line in
128 which only half the standard deviation is added in each case. Additionally, we show two red lines: a solid one
129 capturing the values resulting from subtracting the non-filtered series standard deviation from each of the
130 values of the filtered series, and a dotted one where half the standard deviation is subtracted in each case. In
131 the non-filtered series, where the values are higher than the corresponding dotted blue line, these are
132 considered to be high SIE years for the May series, and where the non-filtered series values are less than the
133 corresponding dotted red line these are regarded as low SIE years for the May series. A list of all the high and
134 low SIE years for the AR by month is shown in the Supplementary Material, together with the high and low
135 SIE years for the main AO subregions, in order to help identify the subregion that most influences the extreme
136 SIE in the AR (Table S1).



137

138 Figure 4 shows the differences between the mean values of MTP for years with low vs high Arctic SIE for
139 each source region (Figure 1a) and for each month. These amounts result from averaging the daily values of
140 MTP, which allows us to estimate the statistical significance by comparing the daily values of MTP for years
141 with years with low and high SIE using a student-t test. A minimum of two months (60 days) and a maximum
142 of 7 months (220 days) are used for the analysis, in either case the student-t test is valid. Table S2 in the
143 supplementary material shows the mean and standard deviation of MTP for minimum and maximum SIE years
144 by month. The results show that for all seasons apart from spring, MTP is greater for years of low ice extent
145 than for those of high extent. The increase in MTP for the minimum SIE years versus the maximum shows a
146 major peak in July and a smaller one in May. For both these months there is agreement between all four
147 moisture sources, the MTP being higher for all of them in July and lower for all of them in May. The summer
148 increase in the MTP is statistically significant for the Atlantic source in June, the Pacific source in August, the
149 Siberian source in June and August, and the North American source in July. In the autumn, the changes in
150 MTP from the different sources are variable, with the MTP from the Atlantic source growing significantly for
151 September and October, but from North America the MTP decreases significantly in September and
152 November but increases in October, in which month the MTP also decreases significantly from the Pacific
153 source. This change in the pattern of MTP does not differ in essence from that observed with the long-term
154 decline of the Arctic SIE (Gimeno-Sotelo et al, 2018) for the autumn, but it is clearly different from that which
155 occurs in the summer, which is characterized by a clear decrease in MTP for the period of low SIE (after 2003)
156 compared with the high-SIE period (before 2003).

157

158 As in Gimeno-Sotelo et al (2018), we compared these results with computations of vertical integrated moisture
159 flux (VIMF) and with an analysis of changes of the frequency of occurrence of the atmospheric circulation
160 types responsible for changes in moisture transport. The use of VIMF can help us to illustrate how moisture
161 is transported from each source to the Arctic, and where the moisture ends up, but it is additionally useful to
162 compare the results of our Lagrangian approach to estimating MTP by checking whether the patterns of
163 differences of VIMF for low versus high SIE years are compatible with the changes we have identified here.
164 Figure 5 shows the composite of differences of VIMF between low and high SIE years for May (results for
165 the remaining months are displayed in Supplementary Figure S2). On inspection of Figure 5, we note that
166 there are no fluxes from the sources to the Arctic; instead they are in the opposite direction, implying that the
167 VIMF is lower for low than for high SIE years in accordance with the results in Figure 3. Results of VIMF
168 analysis for the other months can also explain with almost complete agreement every significant result found
169 from the Lagrangian analysis.



170 The circulation types (CTCs) used in this study are the same as those described in Gimeno-Sotelo et al (2018),
171 based on a approach developed by Fettweis et al. (2011) and shown in Supplementary Figure S3. Changes in
172 the frequency and average MTP of those CTCs linked to high/low MTP can help to corroborate our Lagrangian
173 results. Figure 6, for example, shows the CTCs for Spring together with the average MTP and percentage of
174 occurrence for each CTC for minimum versus maximum SIE years for May. Table S3 in the Supplementary
175 Material shows the MTP averqages for days grouped in each of the CTCs considering minimum and maximum
176 SIE years by month together with the fraction of days in percentage grouped for each CTC. The results of this
177 analysis confirm those from the Lagrangian analysis almost entirely. For the Atlantic source, for example, a
178 change in the frequency of CTC2 is observed for low SIE years (64% of days in May) vs high SIE years (only
179 58.5%) together with a decrease in MTP associated with that CTC, which is coherent with the decrease in
180 MTP for low-SIE years. CTC2 resembles the negative phase of the eastern Atlantic and western Russia
181 (positive height anomalies over the central North Atlantic and negative height anomalies over Europe), linked
182 to enhanced precipitation in the Barents Sea. Thus a decrease in the frequency of this mode would result in
183 reduced MTP for this AO subregion, which is one of the main sinks of the Atlantic source (Gimeno-Sotelo et
184 al, 2018). A similar analysis for the remaining months, sources and CTCs yields results that accord with our
185 Lagrangian analysis.

186

187 ***4.2 The role of extreme events of moisture transport for precipitation on the annual march of the Arctic*** 188 ***sea ice extent***

189 An extreme event of MTP for each of the four moisture sources is defined when there are at least 3 consecutive
190 days with MTP higher than the 75th percentile for the corresponding month. Figure 7 shows histograms of the
191 MTP extremes for each source according to their duration. The highest numbers of events are distributed at
192 the “short” end of the duration, i.e., 3-4 days. This is about 40% of them, with 35% having Atlantic sources
193 (the minimum) and 44% having the Pacific source (the maximum). The number of events decreases
194 significantly as the duration increases, although events lasting a week or more are not infrequent, representing
195 percentages of 16%, 7%, 14%, and 10% for the Atlantic, Pacific, Siberian and North American sources
196 respectively.

197

198 In this paper, a global extreme MTP event (Ext-MTP) takes place when there is temporal concurrence (at least
199 one day) of MTP extreme events from the 4 main sources of moisture for the Arctic. A list of all these events
200 is displayed in the Supplementary Material (Table S2). Because of the marked annual march of the Arctic SIE
201 (Figure 8, blue line with a maximum in mid-March and a minimum in mid-September), the effect of Ext-MTP
202 on this is more evident in the inter-daily change of SIE over two consecutive days (Figure 6, orange line, with



203 negative values from mid-March to mid-September peaking in mid-July and positive values from mid-
 204 September to mid-March peaking in mid-October).

205

206 Figure 9 shows four cases of Ext-MTP, one for each season. The left-hand panel shows the daily change in
 207 SIE together with the extreme MTP periods for each of the sources, shown as horizontal bars in colour. The
 208 periods when these extreme events coincide for three of the sources are shown with a light brown vertical bar,
 209 and the period when all four coincide are shown with dark brown vertical bar; this defines our Ext-MTP. The
 210 green horizontal bars denote the average daily change of SIE before, during, and after the period spanning the
 211 moment when the first extreme of MTP begins for one of the sources and when the last one ends. The effect
 212 that the Ext-MTP has on the daily change of SIE is very clear, producing an increase in winter and a decrease
 213 in spring and summer, and to a lesser degree in autumn. The panel on the right shows the vertical integrated
 214 moisture flux for the day on which the Ext-MTP occurred, and it is clear that the great increase in moisture
 215 transport from the four sources to some Arctic sub-regions is notably higher than the monthly average (Figure
 216 2). Figure S4 in the Supplementary Material shows the results for the 17 Ext-MTP events detected, and
 217 supports conclusions generally similar to those reached for the four example cases.

218

219 5 Links with different fusion mechanisms

220 The impact of MTP on the Arctic SIE is complex and should be understood in terms of the way changes in
 221 precipitation can cause different changes in ice cover associated with different fusion mechanisms depending
 222 on the form of precipitation (rain or snow), as well as its intensity and seasonality. The main contrasting
 223 mechanisms are shown in Table 1 according to season.

224

	Winter	Spring	Summer	Autumn
Snowfall on sea ice	<i>Mechanism 1</i> this enhances thermal insulation reducing sea ice growth (Leppäranta, 1993)	<i>Mechanism 2</i> this increases the surface albedo and thus reduces melting (Cheng et al., 2008)		<i>Mechanism 2</i> is dominant in early Autumn <i>Mechanism 1</i> is dominant in late Autumn
Rainfall on sea ice	<i>Mechanism 3</i> this is related to sea ice melting			
Flooding over the ice	<i>Mechanism 4</i> Both snow and rainfall favour the formation ice superimposed to the ice cover and potentially increase the thickness of the Arctic sea ice			

225

226 *Table 1. Summary of the main contrasting mechanisms of the impact of precipitation on ice cover. Those*
 227 *mechanisms favouring ice-melting are shown in red and those favouring ice growth are shown in blue*



228

229 Figure 10 shows the snowfall fraction obtained from the ERA-interim reanalysis by month for the Arctic
230 region, the Arctic Ocean and the four most important Arctic Ocean subregions in terms of percentage MTP as
231 identified by Gimeno-Sotelo et al (2018): Baffin, Greenland, Bering and Central Arctic. The blue line
232 represents the fraction for high-SIE years and the red line for low-SIE years, the snowfall fraction being higher
233 for high years in almost all months, but especially in summer. The average snow fraction for the year is about
234 0.3 for AR and 0.4 for AO, these values being higher than for the same average for the period from November
235 to May. Regarding the AO subregions, the highest average snow fraction is in the Central Arctic, with almost
236 100% of the precipitation in the form of snow throughout the winter and a good part of the autumn and spring.
237 The lowest proportion occurs in Greenland, where only the winter sees ratios greater than 50%. Therefore, we
238 can say that mechanisms 1 and 2 in Table I relating to precipitation in the form of snow dominate from
239 November to May, and mechanism 3 relating to precipitation in the form of rain dominate from June to
240 October. We are unable to specify the contribution of mechanism 4 relating to the intensity of precipitation
241 and flooding without more detailed data. Albeit in simplistic terms, these essential mechanistic arguments are
242 in agreement with the results presented earlier, suggesting that ice-melting over the two time scales studied
243 here is favoured by an increase in moisture transport in summer, and to a lesser degree in autumn and winter,
244 and a decrease in spring.

245

246 **6 Concluding remarks**

247 In a previous work, Gimeno-Sotelo et al (2018) analysed how the patterns of moisture transport for
248 precipitation varied with the dramatic long-term decline in Arctic ice extent. Using the same region and
249 methodology, we first investigated how the changes in this pattern are linked to the interannual fluctuations
250 that occur in the Arctic ice, superimposed on this decline. The results suggest that ice-melting at this time
251 scale (interannual fluctuations against the trend) is favoured by an increase in moisture transport in summer,
252 and to a lesser degree in autumn and winter, and a decrease in spring. The pattern differs considerably from
253 that found to be linked to decline (Gimeno-Sotelo et al, 2018), especially in summer when it is opposed to it.
254 Then, by exploring the role of extreme MTP events in the Arctic Sea Ice Extent (SIE) we considered what
255 happens to the daily march of the Arctic SIE when extreme MTP arrives simultaneously from the four main
256 moisture regions for the Arctic. The results suggest that on a daily basis the extreme humidity transport for
257 precipitation increases the formation of ice in winter and reduces it in spring, summer and autumn, contributing
258 to melting of the Arctic Sea Ice in these 3 seasons. It is noteworthy that at this time scale, considering the daily
259 change in ice extent, the effect of the MTP on the SIE in summer and autumn is more similar in terms of its
260 effect at the interannual fluctuation scale than at the long-range scale (Gimeno-Sotelo et al, 2018). Thus, in



261 these seasons when the minimum SIE is reached, the ice-melting seems to be favoured by large contributions
262 of MTP at the inter-daily and inter-annual fluctuation scale but not at the long-range scale, suggesting different
263 physical mechanisms that require much deeper study.

264

265 **7 Conflict of Interest Statement**

266 *The authors declare that the research was conducted in the absence of any commercial or financial relationships that*
267 *could be construed as potential conflicts of interest.*

268

269 **8 Author Contributions Statement**

270 LGS performed the calculations and wrote the article, RN design and made the figures, MV provided the
271 MTP data, LG designed the study and wrote the article, and all authors contributed to the interpretation and
272 discussion of the results

273

274 **9 Funding**

275 The authors acknowledge the award by the Spanish government EVOCAR (CGL2015-65141-R) project,
276 which is additionally funded by the European Regional Development Fund (FEDER).

277

278

279 **10 References**

- 280 Cheng, B., Zhang, Z., Vihma, T., Johansson, M., Bian, L., Li, Z. and Wu, H. (2008) Model experiments on
281 snow and ice thermodynamics in the Arctic Ocean with CHINARE2003 data, *J. Geophys. Res.*, 113, C09020,
282 doi:10.1029/2007JC004654.
- 283 Dee, D. P., Uppala, S. M., Simmons, A. J., Berrisford, P., Poli, P., Kobayashi S. and Vitart, F. (2011) The
284 ERA-Interim reanalysis: Configuration and performance of the data assimilation system, *Quarterly Journal*
285 *of the Royal Meteorological Society*, 137(656), 553–597, doi:10.1002/qj.828.
- 286 Dufour, A., Zolina, O. and Gulev, S. K. (2016) Atmospheric Moisture Transport to the Arctic: Assessment of
287 Reanalyses and Analysis of Transport Components, *Journal of Climate*, 29, 5061-5081, doi:10.1175/JCLI-D-
288 15-0559.1.
- 289 Fetterer, F., Knowles, K., Meier, W. and Savoie, M. (2016, updated daily). Sea Ice Index, Version 2. [1979-
290 2016]. Boulder, Colorado USA. NSIDC: National Snow and Ice Data Center, doi:
291 /dx.doi.org/10.7265/N5736NV7. (last accessed 22 November 2017).
- 292 Fettweis, X., Mabilbe, G., Erpicum, M., Nicolay, S. and Van den Broeke, M. (2011) The 1958–2009 Greenland
293 ice sheet surface melt and the mid-tropospheric atmospheric circulation, *Clim. Dynam.*, 36, 139–159,
294 doi:10.1007/s00382-010-0772-8-1.
- 295 Gimeno, L., Dominguez, F., Nieto, R., Trigo, R. M., Drumond, A., Reason, C. and Marengo, J. (2016) Major
296 Mechanisms of Atmospheric Moisture Transport and Their Role in Extreme Precipitation Events, *Annual*
297 *Review of Environment and Resources*, 41, 117–141, doi:10.1146/annurev-environ-110615-085558.
- 298 Gimeno, L., Drumond, A., Nieto, R., Trigo, R. M. and Stohl, A. (2010). On the origin of continental
299 precipitation, *Geophys. Res. Lett.*, 37, doi:10.1029/2010GL043712
- 300 Gimeno, L., Nieto, R., Drumond, A., Castillo, R. and Trigo, R. M. (2013) Influence of the intensification of
301 the major oceanic moisture sources on continental precipitation, *Geophys. Res. Lett.*, 40, 1443–1450,,
302 doi:10.1002/grl.50338
- 303 Gimeno, L., Stohl, A., Trigo, R. M., Domínguez, F., Yoshimura, K., Yu, L., ... Nieto, R. (2012) Oceanic and
304 Terrestrial Sources of Continental Precipitation, *Reviews of Geophysics*, 50, RG4003,
305 doi:10.1029/2012RG000389
- 306 Gimeno-Sotelo, L., Nieto, R., Vázquez, M. and Gimeno L. (2018) A new pattern of the moisture transport for
307 precipitation related to the Arctic sea ice extent drastic decline, *Earth Systems Dynamics*, 9, 611-625,
308 doi:10.5194/esd-9-611-2018.
- 309 Graverson, R. G., Mauritsen, T., Drijfhout, S., Tjernström, M. and Mårtensson, S. (2011). Warm winds from
310 the Pacific caused extensive Arctic sea-ice melt in summer 2007, *Clim. Dynam.*, 36(11), 2103–2112,
311 doi:10.1007/s00382-010-0809-z.
- 312 IPCC: Climate Change (2013). The physical science basis, in: Contribution of working group 1 to the fifth
313 assessment report of the intergovernmental panel on climate change. Edited by: Stocker, T. F., Qin, D.,
314 Plattner, G. K., Tignor, M., Allen, S. K., Boschung, J., Nauels, A., Xia, Y., Bex, V., and Midgley, P. M.,
315 Cambridge University Press, Cambridge, UK and New York, NY, USA,.
- 316 Jakobson, E., Vihma, T., Palo, T., Jakobson, L., Keernik, H. and Jaagus, J. (2012) Validation of atmospheric
317 reanalyses over the central Arctic Ocean, *Geophys. Res. Lett.*, 39, L10802, doi:10.1029/2012GL051591.



- 318 Kapsch, M.-L., Graverson, R. G. and Tjernstrom, M. (2013) Springtime atmospheric energy transport and the
319 control of Arctic summer sea-ice extent, *Nature Climate Change*, 3(8), 744–748, doi:10.1038/nclimate1884
- 320 Leppäranta, M. (1993) A review of analytical models of sea-ice growth, *Atmos. Ocean*, 31, 123–138,
321 doi:10.1080/07055900.1993.9649465.
- 322 Lorenz, C. and Kunstmann, H. (2012) The hydrological cycle in three state-of-the-art reanalyses:
323 Intercomparison and performance analysis, *Journal of Hydrometeorology*, 13, 1397–1420, doi:10.1175/JHM-
324 D-11-088.1
- 325 Numaguti, A. (1999) Origin and recycling processes of precipitating water over the Eurasian continent:
326 Experiments using an atmospheric general circulation model, *J. Geophys. Res. Atmos.*, 104, 1957–1972,
327 doi:10.1029/1998JD200026
- 328 Oshima, K. and Yamazaki, K. (2017) Atmospheric hydrological cycles in the Arctic and Antarctic during the
329 past four decades, *Czech Polar Reports* 7 (2), 169-180, doi: 10.5817/CPR2017-2-17
- 330 Park, H.-S., Lee, S., Son, S.-W., Feldstein, S. B. and Kosaka, Y. (2015) The impact of poleward moisture and
331 sensible heat flux on Arctic winter sea ice variability, *J. Climate*, 28, 5030–5040, doi:10.1175/JCLI-D-15-
332 0074.1
- 333 Roberts, A., Cassano, J., Döscher, R., Hinzman, L., Holland, M., Mitsudera, H., Sumi, A., Walsh, J.E., Alessa,
334 L., Alexeev, V., et al. (2010) A Science Plan for Regional Arctic System Modeling: A Report to the National
335 Science Foundation from the International Arctic Science Community; International Arctic Research Center
336 (IARC): University of Alaska, Fairbanks, AK, USA.
- 337 Stohl, A. and James, P. (2004) A Lagrangian analysis of the atmospheric branch of the global water cycle.
338 Part I: Method description, validation, and demonstration for the August 2002 flooding in central Europe,
339 *Journal of Hydrometeorology*, 5, 656–678, doi:10.1175/1525-7541(2004)0052.0.CO;2.
- 340 Stohl, A. and James, P. (2005) A Lagrangian analysis of the atmospheric branch of the global water cycle.
341 Part II: Moisture transports between the Earth’s ocean basins and river catchments, *Journal of*
342 *Hydrometeorology*, 6, 961–984, doi:10.1175/JHM470.1.
- 343 Vázquez, M., Nieto, R., Drumond, A. and Gimeno, L. (2016) Moisture transport into the Arctic: Source-
344 receptor relationships and the roles of atmospheric circulation and evaporation, *J. Geophys. Res. Atmos.*, 121,
345 doi:10.1002/2016JD025400.
- 346 Vihma, T., Screen, J., Tjernström, M., Newton, B., Zhang, X., Popova, V., Deser, C., Holland, M. and Prowse,
347 T. (2016) The atmospheric role in the Arctic water cycle: A review on processes, past and future changes, and
348 their impacts, *J. Geophys. Res. Biogeosci.*, 121, 586–620, doi:10.1002/2015JG003132.
- 349 Woods, C., Caballero, R. and Svensson, G. (2013) Large-scale circulation associated with moisture intrusions
350 into the Arctic during winter, *Geophys. Res. Lett.*, 40, 4717–4721, doi:10.1002/grl.50912.
- 351 Woods, C. and R. Caballero (2016) The role of moist intrusions in winter Arctic warming and sea ice decline,
352 *Journal of Climate*, 29(12), 4473–4485, doi:10.1175/JCLI-D-15-0773.1.
- 353 Yang, W. and Magnusdottir, G. (2017) Springtime extreme moisture transport into the Arctic and its impact
354 on sea ice concentration, *J. Geophys. Res. Atmos.*, 122, 5316–5329, doi: 10.1002/2016JD026324.
- 355 Zhang, X., He, J., Zhang, J., Polyakov, I., Gerdes, R., Inoue, J. and Wu, P. (2012) Enhanced poleward moisture
356 transport and amplified northern high-latitude wetting trend, *Nature Climate Change*, 3, 47–51,
357 doi:10.1038/nclimate1631



358 **Captions**

359 **Figure 1.** A) The Arctic region (AR) using the definition of Roberts et al. (2010) together with the major
360 moisture sources for the Arctic as detected by Vazquez et al. (2016). B) The Arctic Ocean (AO) and its main
361 subregions

362 **Figure 2.** Climatological values of the vertical integrated moisture flux (VIMF) (vector, $\text{kg m}^{-1} \text{s}^{-1}$) for the
363 first month of each season together with the main Arctic sources identified by Vázquez et al (2016), the AR
364 and the main sub-regions of the AO in terms of moisture received from the source regions

365 **Figure 3.** Extreme years for May Arctic SIE.

366 **Figure 4.** Differences between mean values of Moisture transport for precipitation (MTP) (mm day^{-1}) for
367 years with low vs high Arctic SIE for each source region. Filled bars show differences that are statistically
368 significant at the 95% confidence level.

369 **Figure 5.** Composite of differences of vertical integrated moisture flux (VIMF) (vector, $\text{kg m}^{-1} \text{s}^{-1}$) between
370 low and high SIE years for May. The AR, the main moisture sources regions and the main AO subregions are
371 also displayed.

372 **Figure 6.** (right) Anomalies of geopotential height at 850 hPa (Z850) for the four types of circulation centred
373 in the four source sectors (classes CTC1 to CTC4) for Spring (left) The average MTP and percentage of
374 occurrence for each CTC for minimum SIE years versus the maximum in May.

375 **Figure 7.** Histograms of the Moisture transport for precipitation (MTP) extremes for each source according
376 to their duration

377 **Figure 8.** SIE annual march (blue line) and SIE inter-daily change (orange line).

378 **Figure 9.** Four selected cases of Ext-MTP (mm day^{-1}), one for each season. (Left panel) Daily change of SIE
379 (black line), extreme MTP periods for each of the sources (horizontal bars in colour), Coincident extreme
380 MTP for the sources (light brown vertical bar shows when there are three coincident MTPs, dark brown
381 vertical bar when there are four coincident MTPs), averages of the daily change of SIE for different periods
382 (green horizontal bars). (Right panel) vertical integrated moisture flux plotted for the day on which the Ext-
383 MTP occurred.

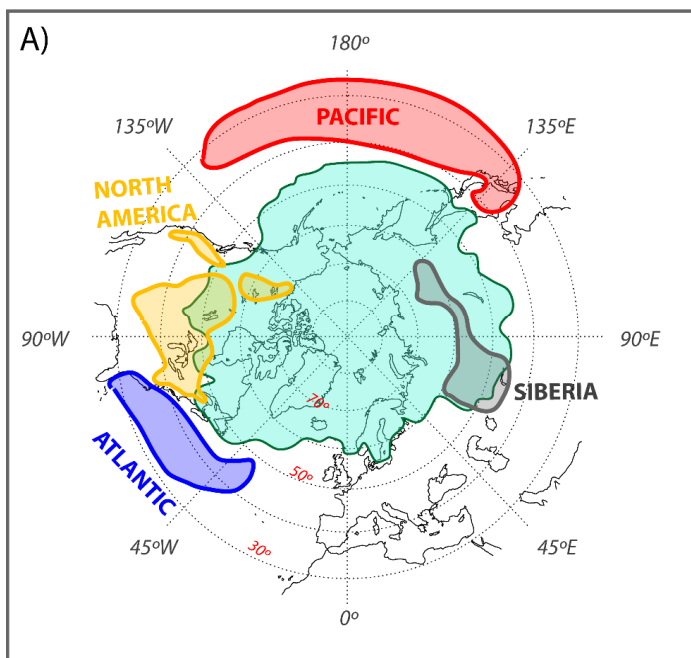
384 **Figure 10.** Snowfall fraction taken from the ERA-interim reanalysis by month for the AR, the AO and the
385 four more important AO subregions in terms of percentage of MTP as identified by Gimeno-Sotelo et al
386 (2018): Baffin, Greenland, Bering and Central Arctic. Blue line represents the fraction for high SIE years and
387 red line for low SIE years, the snowfall fraction being higher for high years in almost all months but especially
388 in summer.

389

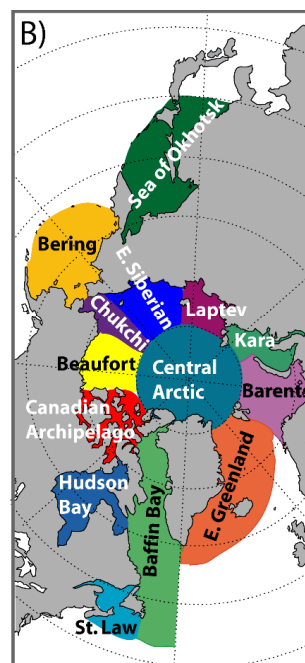
390



ARCTIC SYSTEM & ITS MAIN MOISTURE SOURCES



SEAS of the ARCTIC OCEAN



398

399

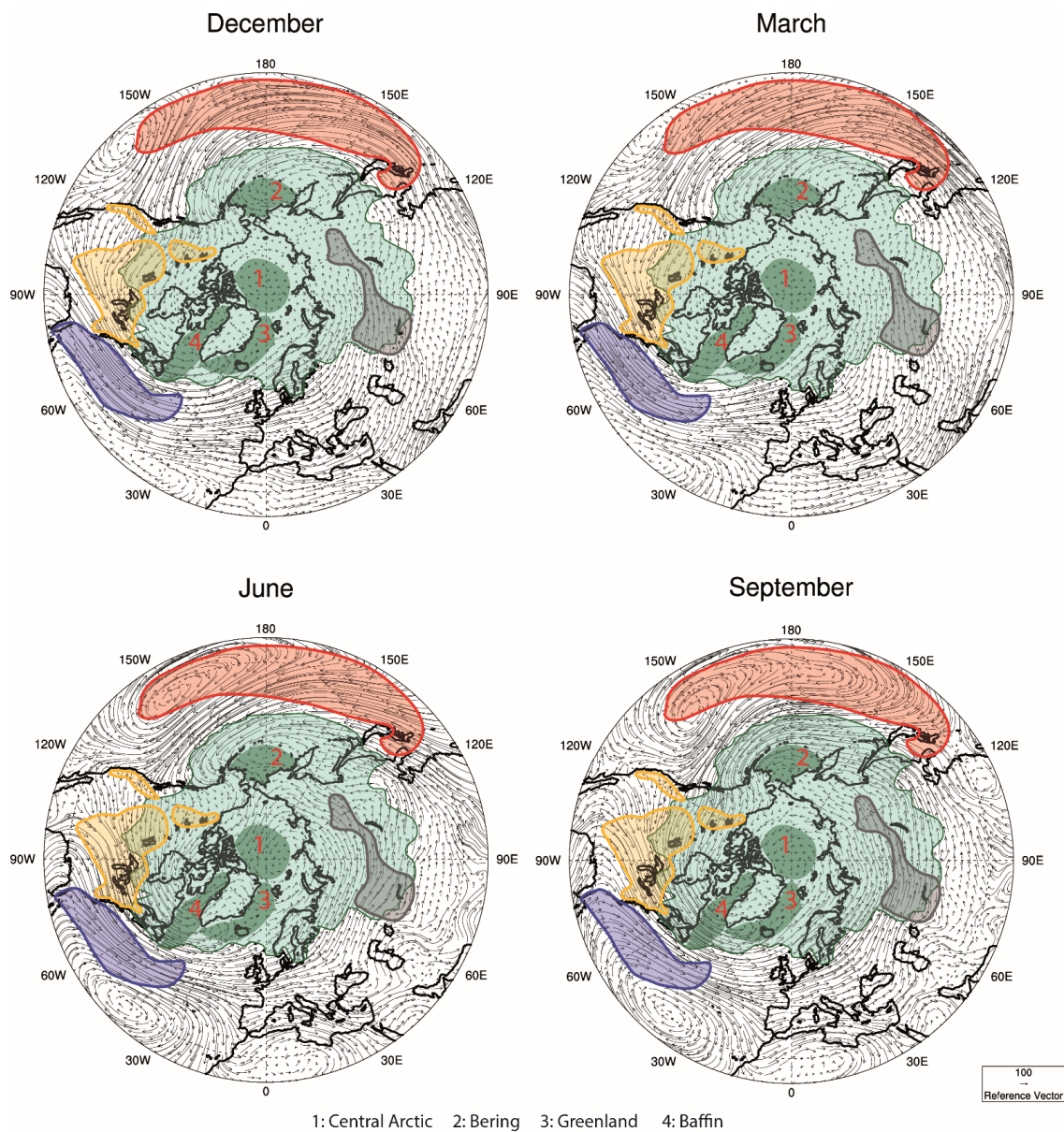
400 **Figure 1**

401

402



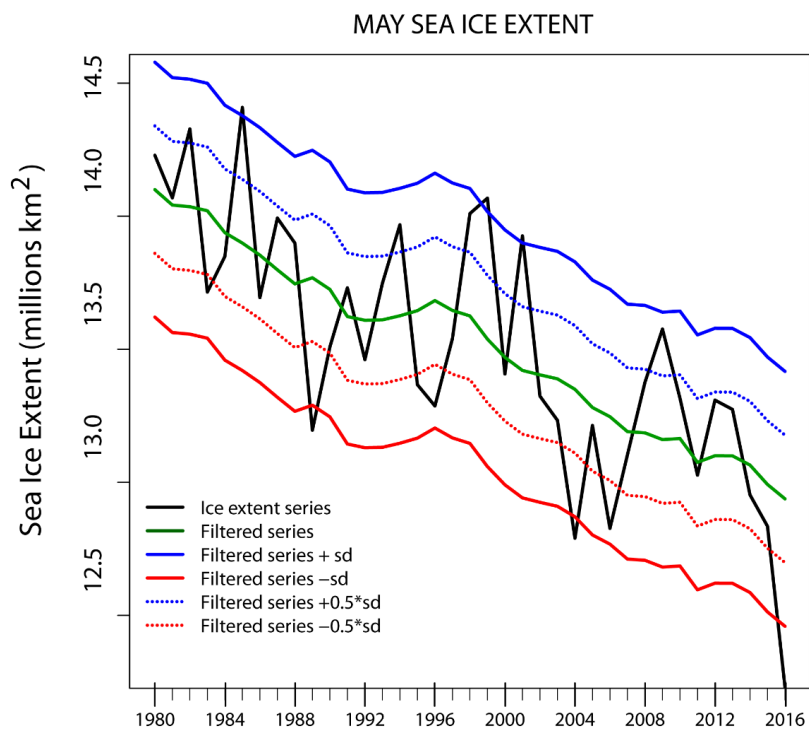
403



404

405 **Figure 2**

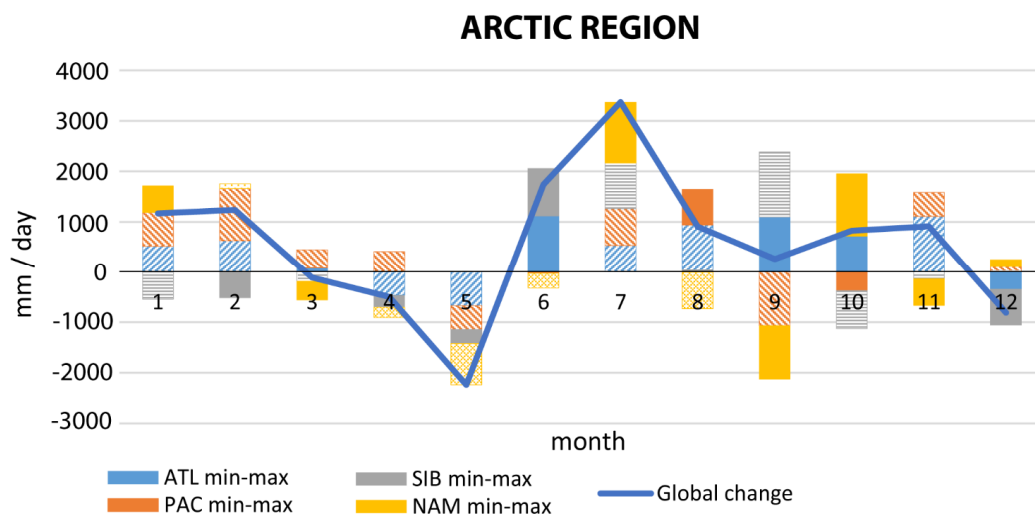
406



407

408 **Figure 3**

409



410

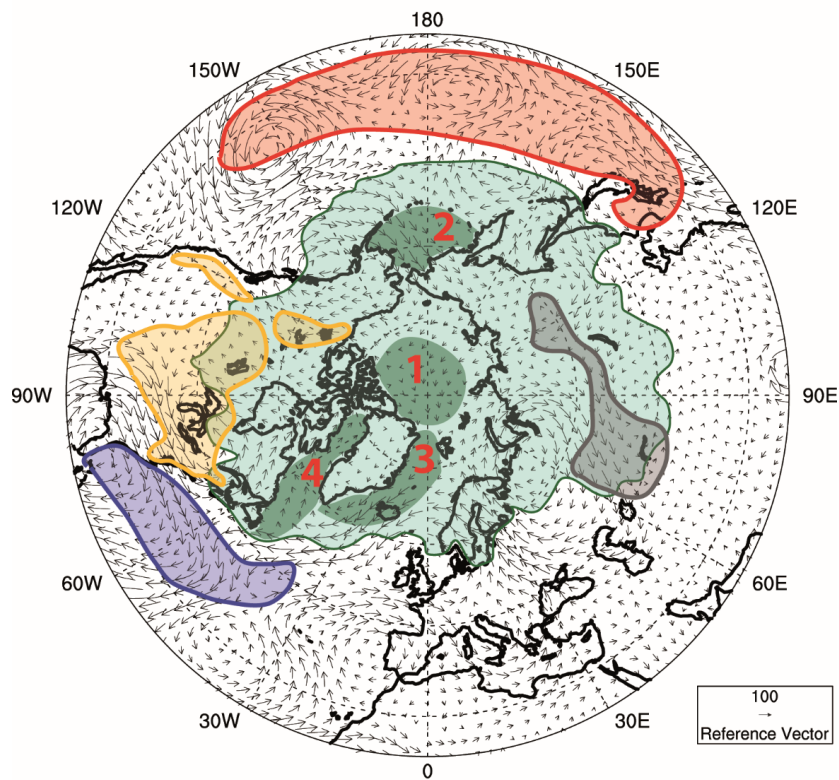
411 **Figure 4**

412



MAY

VIMF differences between MIN and MAX SIE

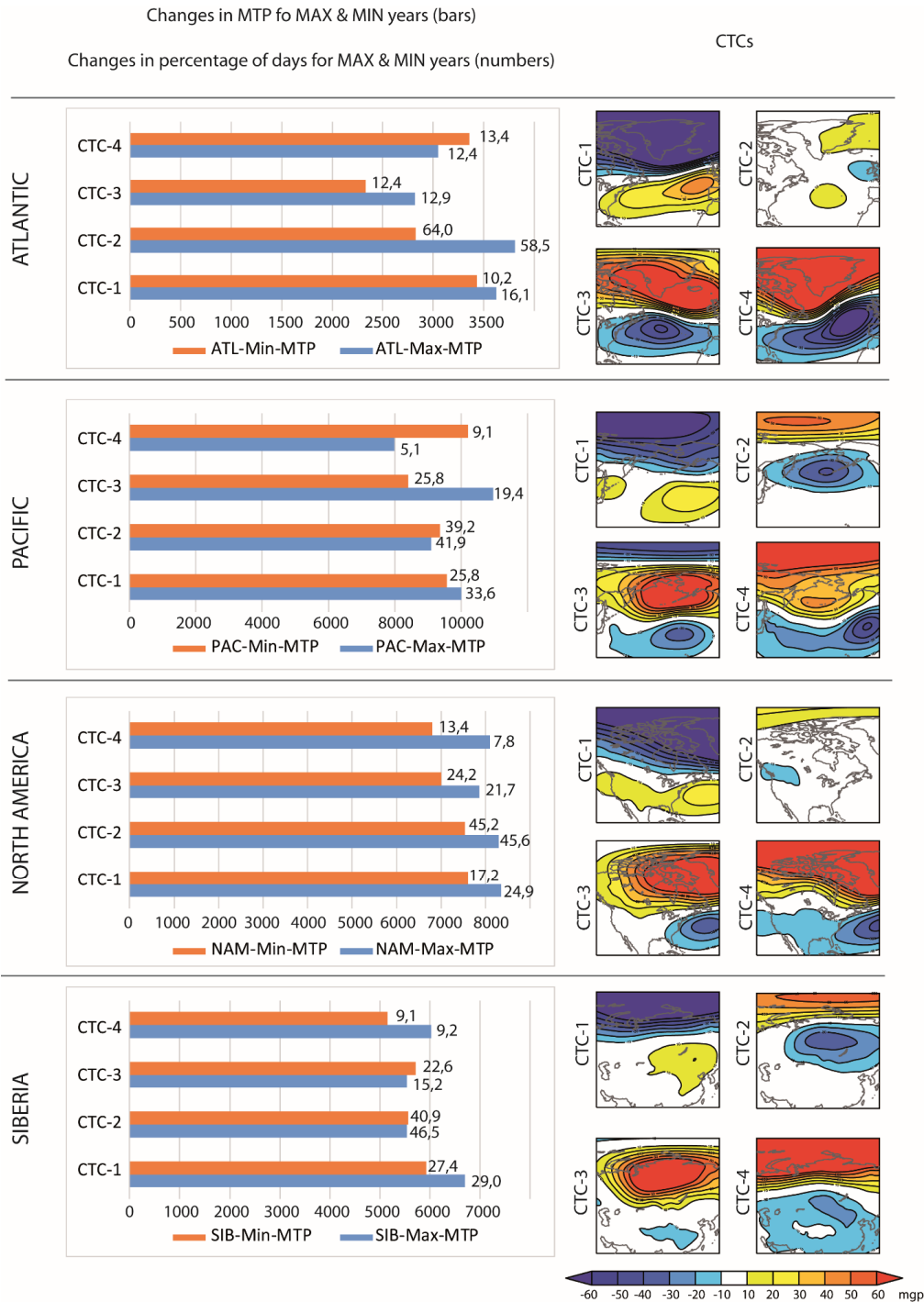


1: Central Arctic 2: Bering 3: Greenland 4: Baffin

413

414 **Figure 5**

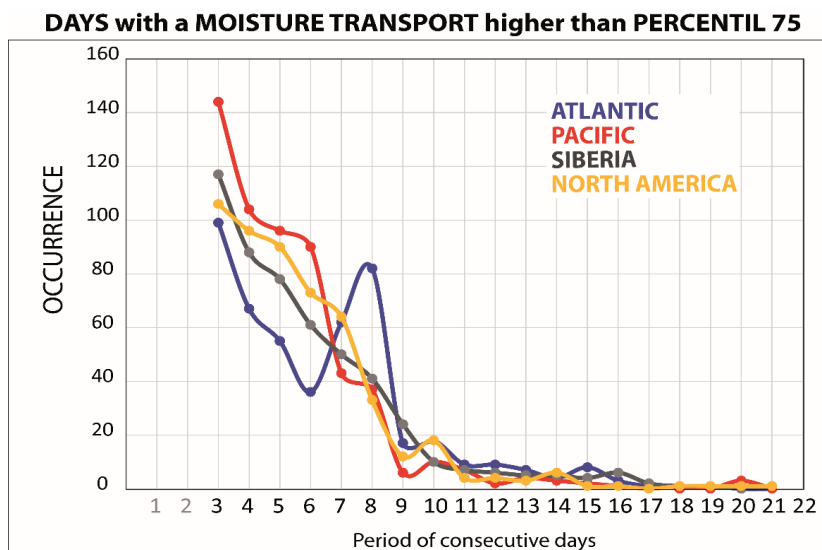
415



416

417 **Figure 6**

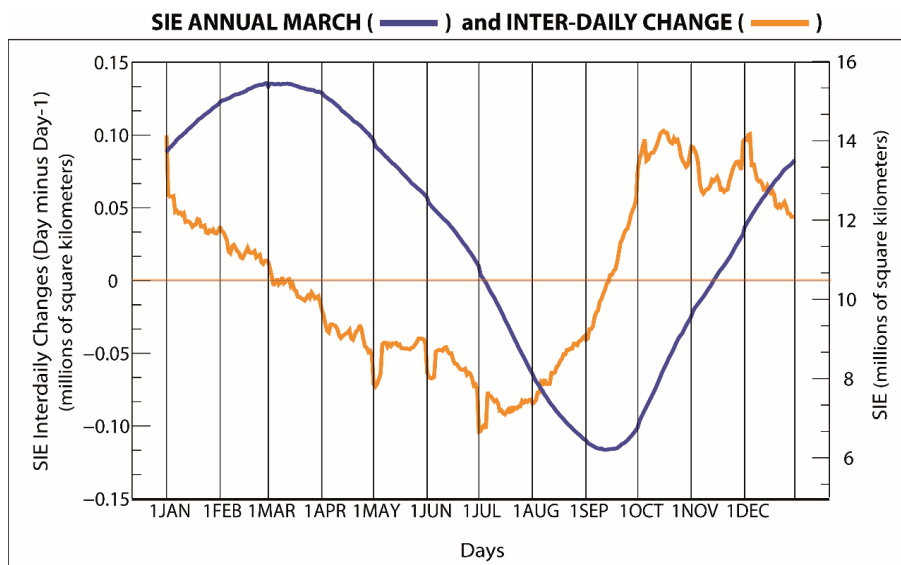
418



419

420 **Figure 7**

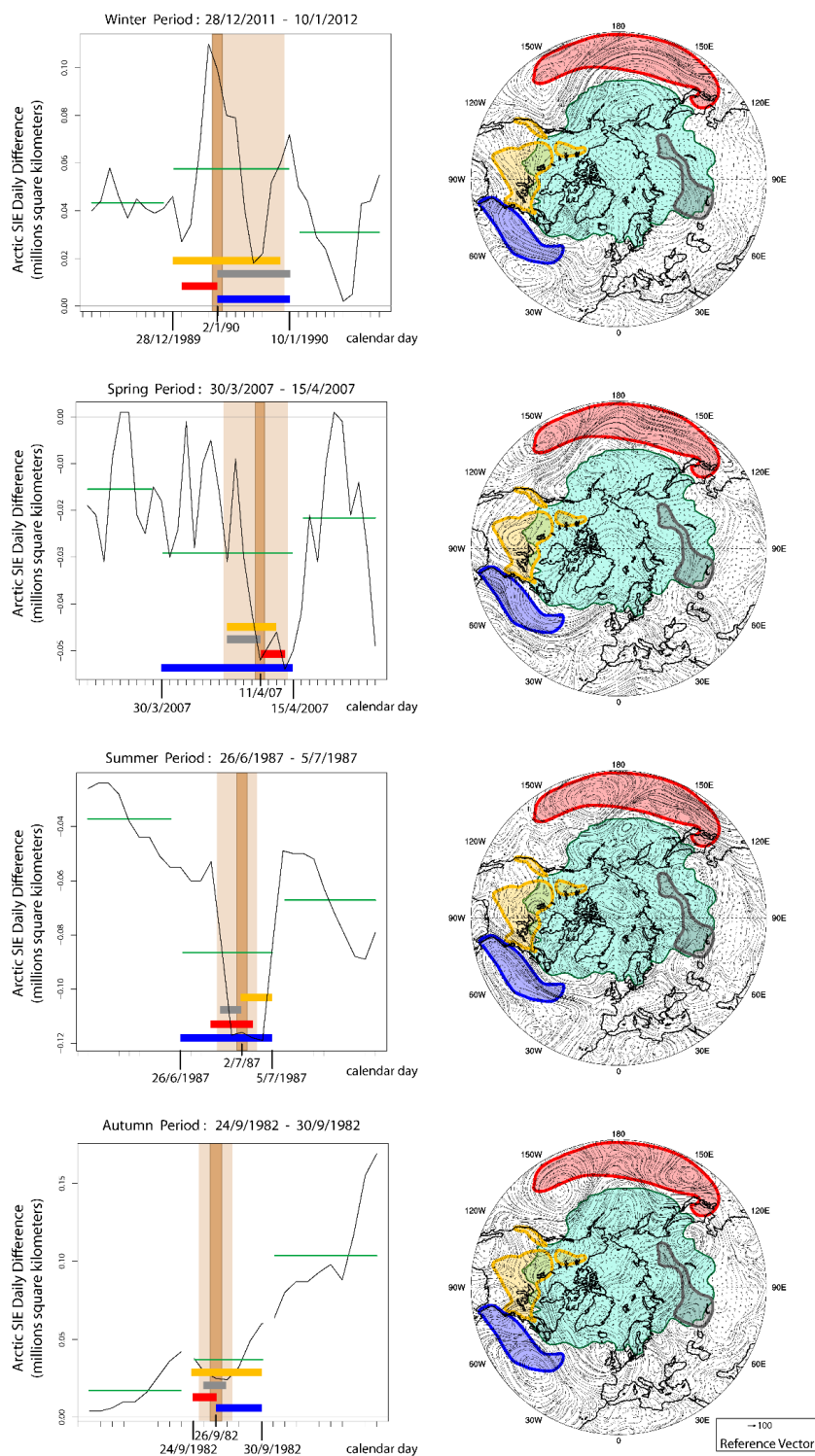
421



422

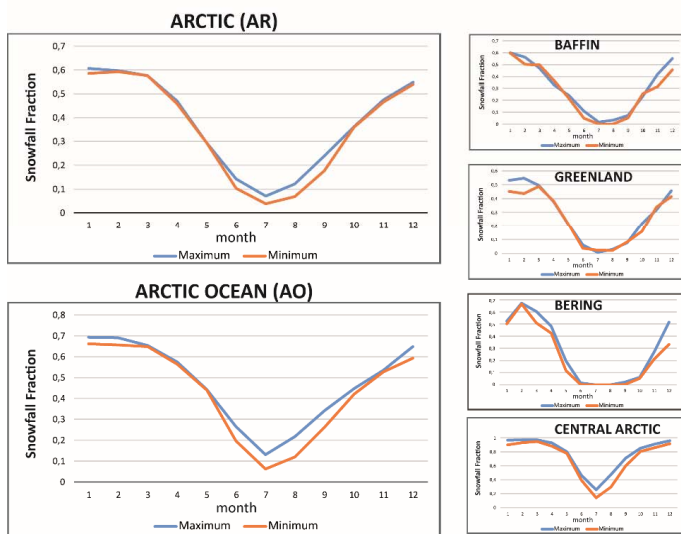
423 **Figure 8**

424



425

426 **Figure 9**



427

428 **Figure 10**

429